BIOCHEMISTRY
including biophysical chemistry & molecular biology
Article

Biochemistry **2010,** *49,* 2741–2752 2741
DOI: 10.1021/bi902137c

Site-Specific Effects of Diselenide Bridges on the Oxidative Folding of a Cystine Knot Peptide, ω-Selenoconotoxin GVIA†

Konkallu Hanumae Gowd,‡ Viktor Yarotskyy,⊥ Keith S. Elmslie,⊥ Jack J. Skalicky,§ Baldomero M. Olivera,‡ and Grzegorz Bulaj*,∥

‡*Departments of Biology,* §*Biochemistry, and* ∥*Medicinal Chemistry, University of Utah, Salt Lake City, Utah 84108, and* ⊥*Department of Anesthesiology and Pharmacology, Penn State College of Medicine, Hershey, Pennsylvania 17033*

Received December 13, 2009; Revised Manuscript Received February 15, 2010

ABSTRACT: Structural and functional studies of small, disulfide-rich peptides depend on their efficient chemical synthesis and folding. A large group of peptides derived from animals and plants contains the Cys pattern C−C−CC−C−C that forms the inhibitory cystine knot (ICK) or knottin motif. Here we report the effect of site-specific incorporation of pairs of selenocysteine residues on oxidative folding and the functional activity of ω-conotoxin GVIA, a well-characterized ICK-motif peptidic antagonist of voltage-gated calcium channels. Three selenoconotoxin GVIA analogues were chemically synthesized; all three folded significantly faster in the glutathione-based buffer compared to wild-type GVIA. One analogue, GVIA[C8U,C19U], exhibited significantly higher folding yields. A recently described NMR-based method was used for mapping the disulfide connectivities in the three selenoconotoxin analogues. The diselenide-directed oxidative folding of selenoconotoxins was predominantly driven by amino acid residue loop sizes formed by the resulting diselenide and disulfide cross-links. Both *in vivo* and *in vitro* activities of the analogues were assessed; the block of N-type calcium channels was comparable among the analogues and wild-type GVIA, suggesting that the diselenide replacement did not affect the bioactive conformation. Thus, diselenide substitution may facilitate oxidative folding of pharmacologically diverse ICK peptides. The diselenide replacement has been successfully applied to a growing number of bioactive peptides, including α-, μ-, and ω-conotoxins, suggesting that the integrated oxidative folding of selenopeptides described here may prove to be a general approach for efficient synthesis of diverse classes of disulfide-rich peptides.

Multiple disulfide cross-links are a major structural feature of many secreted polypeptides (*1*−*3*). If a secreted polypeptide is injected or meant to act on another organism (as is the case for animal venom components), it is subject to an additional selective pressure: to make the polypeptide smaller for rapid dissemination through the targeted animal's body. There is likely also selection for a tighter, less flexible structure to increase resistance to proteases, presumably leading to an even higher degree of disulfide cross-linking. Thus, most animal venom polypeptides characterized, independent of their phylogenetic origin, are significantly smaller and much more disulfide rich than other polypeptides (*4*). This evolutionary trend reaches a zenith in some *Conus* venoms, where 12 amino acid residue venom peptides with three disulfide cross-links have been identified (*5*). There is also an increasing pharmacological interest in disulfide-rich peptides, not only because they are often highly selective in their targeting specificity but also because of their potential as templates for drug development (*6*, *7*).

A general problem encountered when working with small, disulfide-rich peptides is that they can be difficult to fold *in vitro* (*8*−*11*). A peptide with three disulfide bonds can potentially form 15 isomers, each with different cross-links. Thus, achieving a good yield of the properly folded, biologically active peptide can be a significant challenge. Indeed, some peptides have never been successfully folded (although failures are rarely reported in the literature). Replacing disulfide bridges with diselenide bridges turned out to be an effective strategy to simplify oxidative folding of cysteine-rich peptides without affecting their native conformation or biological activity (*12*−*16*). The greater redox stability and more rapid formation of diselenide bonds, as compared to disulfide bonds, can be used to significantly improve folding yields. Furthermore, a new approach to facilitate folding and simultaneously improve disulfide mapping (i.e., "integrated oxidative folding") was recently introduced (*16*). The basic strategy is to substitute a diselenide for one disulfide cross-link in a peptide containing a pair of $^{13}C/^{15}N$-labeled cysteine residues. Although promising with respect to engineering oxidative folding of peptides containing multiple disulfide bridges, the selenopeptide strategy has been tested on very few disulfide-rich motifs.

A particularly common motif in small polypeptides with three disulfide bonds is the inhibitory cysteine knot (ICK)[1] or knottin motif, with one disulfide bond threaded through the other two,

†This work was supported by the NIH program project PO1 GM-49677. The electrophysiology was supported by a grant from the Pennsylvania Department of Health using Tobacco Settlement Funds.

*Address correspondence to this author: phone, (801) 581-4629; fax, (801) 581-7087; e-mail, bulaj@pharm.utah.edu.

[1]Abbreviations: $Ca_V2.2$, N-type calcium channel; DTT, dithiothreitol; FT-MS, Fourier transform mass spectrometry; GVIA, ω-conotoxin GVIA; GSH, reduced glutathione; GSSG, oxidized glutathione; ICK, inhibitory cystine knot; NOESY, nuclear Overhauser enhancement spectroscopy; RP-HPLC, reverse-phase high-performance liquid chromatography; Sec, selenocysteine; Sec-GVIA, selenocystine containing GVIA.

Published on Web 02/22/2010

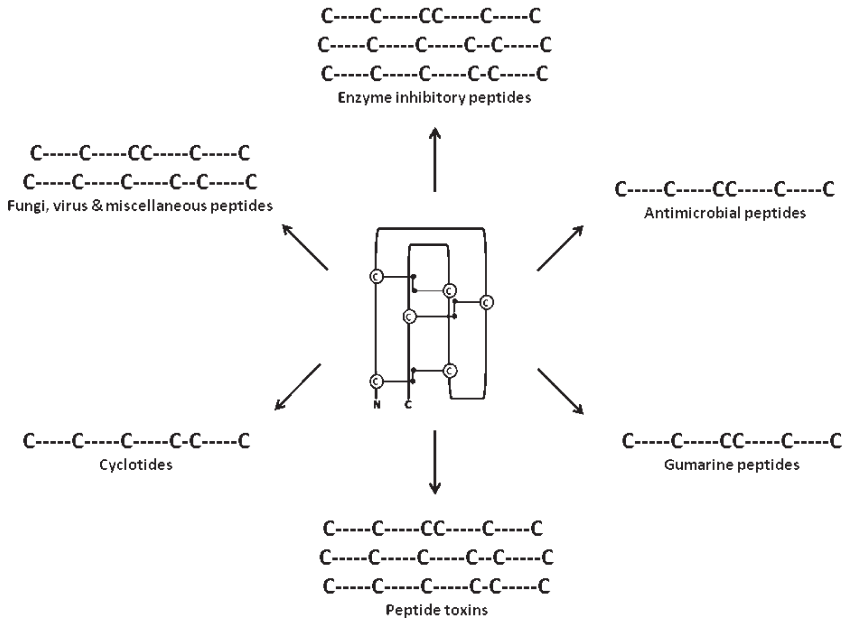

FIGURE 1: Inhibitory cysteine knot (ICK) motif and available cysteine patterns in three disulfide-containing peptides as revealed from KNOTTIN database analysis (see Supporting Information Table S1 for details). The KNOTTIN database, standardized database of ICK motifs, contains 1621 sequences out of which > 1000 sequences possess six cysteines. ICK peptides containing six cysteine residues can be further classified into three types based on cysteine pattern in the sequence. Greater than 750 sequences in the database share the following cysteine pattern: C---C---CC---C---C, identical to ω-conotoxin GVIA.

thereby forming a topological knot (*17*−*20*). The three hydrophobic disulfide bonds generally constitute the hydrophobic interior of the polypeptide, greatly stabilizing the ICK structural framework (*18*, *21*). Figure 1 and Supporting Information Table 1 summarizes the diversity of ICK motif and corresponding occurrence of cysteine patterns in three disulfide-containing peptides. The cysteine pattern C---C---CC---C---C is shared by various peptides including those isolated from microbes, insects, plants, and animals and can be considered currently the largest class within the ICK motif family. This motif is shared by one well-characterized class of *Conus* snail venom peptides (*22*). The O-gene superfamily of conopeptides has differentiated into a number of pharmacologically distinct families, each with different targeting specificity. This is a consequence of the unprecedented rate of evolution of conopeptide superfamilies (*23*, *24*).

Among the ICK motif *Conus* peptide families are the ω-conopeptides that inhibit voltage-gated calcium channels (*25*), the κ-conopeptides that target voltage-gated K channels (*26*), the δ-conopeptides that inhibit voltage-gated Na channel inactivation (*27*) ,and the μO-conotoxins that inhibit Na channel activation (*28*, *29*). Arguably, the best characterized of all of the O-superfamily peptides are the members of the ω-family that block voltage-gated Ca^{2+} channels (*30*, *31*). One of these, ω-conotoxin MVIIA, is an approved drug for intractable pain (Prialt) (*32*, *33*). Perhaps the most widely used disulfide-rich peptide in neuroscience is ω-conotoxin GVIA (*30*, *31*, *34*, *35*), which was key to the identification and biochemical characterization of N-type Ca channels ($Ca_V2.2$) (*36*−*38*) and has become a standard pharmacological tool for inhibiting synaptic transmission (*39*, *40*). The oxidative folding of ω-conotoxins was previously investigated by Goldenberg and co-workers (*41*−*44*). These peptides are generally more easily folded *in vitro* than some other *Conus* peptides, although folding yields for ω-conotoxins can be also relatively low (*41*).

In this report, we applied the integrated oxidative folding strategy to ω-conotoxin GVIA: selenoconotoxin GVIA analogues containing a pair of $^{13}C/^{15}N$-labeled cysteines were synthesized, and their folding and bioactivity were investigated. The solution structure, disulfide bridging pattern, and folding properties of GVIA are well established (*45*−*48*). Because the interactions of GVIA with its target, N-type Ca channels, have been extensively characterized (*49*−*53*), an assessment of the effects of substituting a diselenide for a particular disulfide cross-link can be carried out with an unprecedented sensitivity. Our results suggest that there are significant differences in the kinetics of folding as the single diselenide-bonded analogues are folded to the corresponding fully oxidized diselenide-containing GVIA species. This is the first report on applying the integrated oxidative folding to the ICK peptides, suggesting a broader applicability of this strategy toward discovery efforts and studying structure/function of diverse disulfide-rich peptides.

EXPERIMENTAL PROCEDURES

Peptide Synthesis. Peptides were synthesized using standard Fmoc (*N*-(9-fluorenyl)methoxycarbonyl) chemistry and activated Opfp (pentafluorophenyl) esters of the protected amino acids, as described (*16*). Side chains of selenocysteines were protected with a *p*-methoxybenzyl group (Chem Impex Int., Wood Dale, IL), labeled cysteines (U-$^{13}C3$, 97−99%; ^{15}N, 97−99%; Cambridge Isotope Laboratories, Andover, MA) and unlabeled cysteines were protected with trityl (Trt) groups, and 4-hydroxyproline was protected with a tBu group. Sec-GVIA analogues were removed from the resin using enriched reagent K [trifluoroacetic acid (TFA)/thianisol/phenol/water (90:2.5:7.5:5) and 1.3 equiv of DTNP (2,2′-dithiobis(5-nitropyridine))], and GVIA was cleaved using reagent K [TFA/thianisol/phenol/water/ethanedithiol (82.5:5:5:5:2.5)]. Peptides were precipitated with methyl *tert*-butyl ether (MTBE) and washed several times with cold MTBE. Sec-GVIA analogues were subjected to DTT (*threo*-1,4-dimercapto-2,3-butanediol) treatment, before purification, using 50 mM DTT in 100 mM Tris-HCl (pH 7.5) containing 1 mM EDTA for 1 h, as described (*16*). Peptides

were purified using preparative RP-HPLC using a C_{18} column over a linear gradient of 10−35% buffer B (90% acetonitrile containing 0.1% TFA) for 40 min. Purified peptides were analyzed using mass spectrometry. The observed mass of Sec-GVIA analogues is 2 Da less than predicted mass, confirming the presence of diselenide in the peptide (expected, 3145 Da; observed, 3143 Da).

Previous studies with μ-selenoconotoxin SIIIA proved that, after an aforementioned cleavage/reduction method, the peptide analogues contained a preformed diselenide bridge, as deducted from mass spectrometry analysis of the alkylation products (*16*). To confirm the presence of a diselenide bridge in the "linear" form of Sec-GVIA prior to the folding experiments, one of the analogues, GVIA[C8U,C19U] was subjected to the alkylation reaction, followed by mass spectrometry analysis (Figure S1, Supporting Information). First, the crude, postcleavage peptide was shown to contain two 5-thionitropyridyl groups (Figure S1, Supporting Information). After thiolysis with DTT and subsequent alkylation with iodoacetamide, the resulting species was shown by mass spectrometry to contain a diselenide bridge. HPLC traces, mass spectra, and experimental details are provided in the Supporting Information.

Oxidative Folding. Folding reactions were initiated by resuspending 5 nmol of linear peptides into 200 μL of folding buffer containing 0.1 M Tris-HCl (pH 7.5), 1 mM EDTA, 1 mM oxidized glutathione (GSSG), and 2 mM reduced glutathione (GSH). Reaction was quenched, after an appropriate time interval, by acidification with formic acid (10% final concentration). Samples were further analyzed using C_{18} analytical HPLC over a linear gradient of 10−40% buffer B (90% acetonitrile containing 0.1% TFA) in 40 min. Accumulation of natively folded peptide at a given time point was calculated by integrating the HPLC chromatogram. Two Sec-GVIA analogues have nearly the same retention time for folded and linear peptides; in such cases, the isotopic patterns of observed and predicted masses were compared, and the quality of folded peptides was accessed. At all of the given time intervals, the observed isotopic pattern was similar to the predicted peptide, confirming the presence of folded peptide. (Note: the most intense peaks of linear and folded peptides in the mass spectrum have the same charge stated: $[M + 4H]^{4+}$.) Experimental points were analyzed by Prism software (GraphPad Software, Inc., San Diego, CA), and the rate constant was calculated by a single exponential fit. Oxidative folding experiments in the presence of denaturing agent, 8 M urea, were carried out as described above.

Mass Spectrometry and NMR Spectroscopy. Electrospray ionization (ESI) mass spectra were obtained using a Micromass Quattro II mass spectrometer at the Mass Spectrometry and Proteomics Core Facility of the University of Utah. ESI-FTMS was recorded using Thermo-FT-MS, and data were analyzed using the software provided by the manufacturer. A theoretical isotopic pattern of Sec-GVIA was derived using the molecular formula $C_{114}H_{190}N_{36}O_{43}S_4Se_2Z_6X_2$, where Z = ^{13}C and X = ^{15}N. Sec-GVIA analogues for NMR were prepared by dissolving purified peptide (1 mM) in buffer containing 40 mM sodium phosphate (pH 6.2), 50 mM sodium chloride, 90% H_2O, and 10% D_2O. Two-dimensional [^{13}C,^{1}H] HSQC and 2D [^{1}H,^{1}H] ^{13}C-edited NOESY were recorded at 15 °C on a Varian Inova 600 NMR spectrometer with a cryogenic probe. Data were processed with FELIX2004 and analyzed using the SPARKY program (T. D. Goddard and D. G. Kneller, University of California, San Francisco).

Disulfide Mapping of Non-Native Folded Species. The non-native folded species of GVIA[C1U,C16U] and GVIA[C15U,C26U] were isolated after reaching the steady state during oxidative folding in the presence of 8 M urea. Disulfide mapping of GVIA[C1U,C16U] was achieved through proteolysis using trypsin and GVIA[C15U,C26U] using chymotrypsin. Five nanomoles of the peptide was dissolved in 100 mM sodium phosphate buffer of pH 6.8 and incubated with the desired enzyme for 24 h at 37 °C. The enzyme to substrate ratio was 1:100. The resulting proteolytic fragments were separated using an analytical C_{18} HPLC column over the linear gradient of acetonitrile from 10% to 50% over 40 min. Isolated peptide fragments were characterized using MALDI-MS, and the topology of corresponding non-natively folded peptide was deduced.

Measurement of N-Type Calcium Currents (*CaV2.2*). HEK293 cells were transfected as previously described with $Ca_V2.2_{-CFP}$, $\alpha_2\delta$ and β_{2a} subunits (*54*). N-channel expressing cells were visualized by CFP (cyan fluorescent protein), which was attached to the N-terminus of α_{1B} ($Ca_V2.2_{-CFP}$). Cells were voltage-clamped using the whole-cell configuration of the patch clamp technique as described previously (*54*, *55*). The external recording solution contained 5 mM $BaCl_2$, 145 mM *N*-methyl-D-glucamine (NMG)-Cl, and 10 mM NMG-HEPES, osmolarity = 325 mOsm and pH = 7.4. The pipet solution contained 104 mM NMG-Cl, 10 mM NMG-HEPES, 10 mM NMG-EGTA, 6 mM $MgCl_2$, 5 mM Tris-ATP, 0.3 mM Tris-GTP, and 14 mM creatine phosphate, osmolarity = 280 mOsm and pH = 7.4. Wild-type ω-conotoxin GVIA for the electrophysiology experiments was purchased from Bachem Americas (King of Prussia, PA). Test solutions were applied from a gravity-fed perfusion system with an exchange time of 1−2 s. Group data were calculated as mean ± SD, and significance differences ($p < 0.05$) were determined using a one-way ANOVA with Tukey HSD *post hoc* analysis.

Behavioral Assay. Intracerebral injection of folded GVIA and Sec-GVIA analogues to 21−23-day-old Swiss Webster mice was achieved using a syringe with a 29-gauge needle. Mice injected with equal volumes of normal saline were used as control. After injection, mice were placed in a cage for observation. All of the peptides exhibited shaking syndrome, which is characterized by persistent body tremor, and this behavior maintained for a long time period in a dose-dependent manner (*25*).

RESULTS

Chemical Synthesis. To study the effects of site-specific incorporation of diselenide bridges, three GVIA analogues were designed and synthesized, namely, GVIA[C1U,C16U], GVIA[C8U,C19U], and GVIA[C15U,C26U]. Each analogue had a single native disulfide bridge replaced by a diselenide bridge (Figure 2). Incorporation of selenocystine was achieved by introducing *p*-methoxybenzyl-protected selenocysteine during solid-phase peptide synthesis.

After cleavage, the crude peptide was subjected to 50 mM DTT treatment (thiolysis) to enrich for the reduced selenoconotoxin analogue (*16*). The predicted reduced peptide mass of the Sec-GVIA analogues is 3145.2 Da, and observed masses for GVIA[C1U,C16U], GVIA[C8U,C19U], and GVIA[C15U,C26U] were 3143.2, 3143.3, and 3143.2 Da, respectively. The observed mass for all the reduced Sec-GVIA analogues was 2 Da less than the predicted mass, consistent with the presence of a preformed diselenide bridge. Mechanistic features underlying deprotection

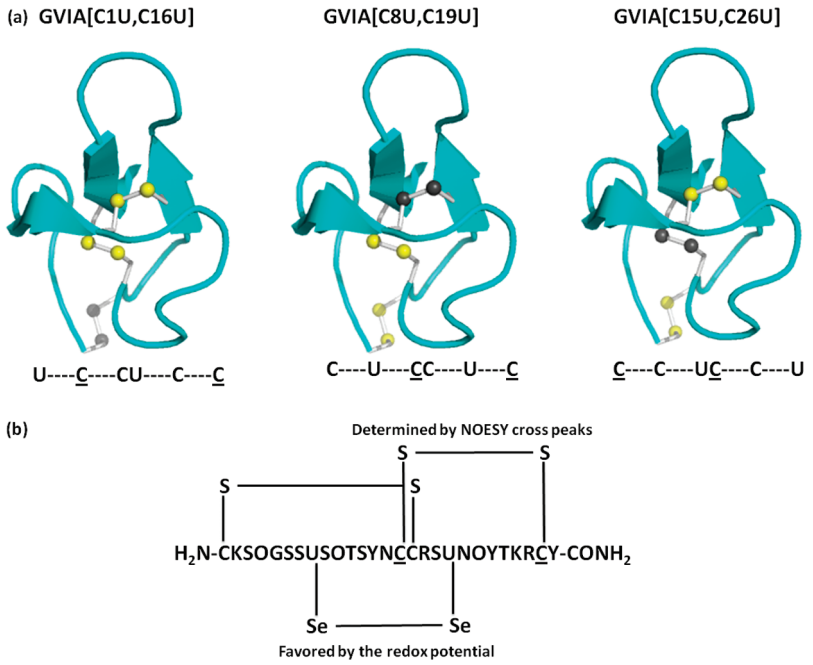

FIGURE 2: Structural representation of Sec-GVIA analogues and the strategy for disulfide mapping using the integrated oxidative folding. (a) The position of the distinct diselenide bond in the 3D structure of GVIA (diselenide bond in gray and disulfide bond in yellow) and corresponding cysteine/selenocysteine patterns (U and C correspond to selenocysteine and $^{13}C/^{15}N$-labeled cysteine residues, respectively). The structure of GVIA (2CCO) was modeled using PyMOL software. (b) The integrated oxidative folding strategy using GVIA[C8U,C19U]. The redox potential favors diselenide (−381 mV) over selenosulfide (−326 mV), whereas the labeled cysteine residues facilitate NMR-based disulfide mapping by identification of cross-disulfide NOEs.

of the selenocysteine side chain protecting group by DTNP (*56*, *57*) and the low redox potential of diselenide (E_o = −381 mV) over disulfide (E_o = −180 mV) and selenosulfide (E_o = −326 mV) with respect to DTT (E_o = −323 mV) (*58*) predicted the presence of the preformed diselenide in the reduced Sec-GVIA analogues, which was actually detected (Figure S1, Supporting Information).

The diselenide-containing reduced Sec-GVIA analogues were subjected to oxidative folding with a mixture of oxidized (1 mM GSSG) and reduced (2 mM GSH) glutathione; these folding conditions were shown previously to promote efficient folding of GVIA (*41*). Figure 3a shows chromatographic elution profiles of the oxidative folding of GVIA and Sec GVIA analogues at the steady state. The identity of folded species was further characterized using mass spectrometry and NMR. Figure 3b shows steady-state accumulation of natively folded GVIA and Sec-GVIA analogues during oxidative folding. The order of highest accumulation of natively folded peptides for Sec-GVIA analogues is GVIA[C8U,C19U] > GVI[C1U,C16U] > GVIA[C15U,C26U]. The folding efficiency of GVIA and GVIA[C15U,C26U] was found to be nearly the same. Diselenide in the second position of the canonical disulfide connectivity of ω-conotoxin GVIA has a greater influence on improving the folding efficiency to yield the native configuration.

For GVIA[C1U,C16U] and GVIA[C15U,C26U], the folded and reduced species exhibited identical HPLC retention times. In order to access the quality of folded peptides, high-resolution FT-MS was employed, and the isotopic pattern generated from elemental composition was compared to that of the observed peptide isotopic pattern. Supporting Information Figure S2 shows the high-resolution FT mass spectrum of folded GVIA-[C1U,C16U] and the corresponding theoretical spectrum. The isotopic patterns of the theoretical and experimental mass spectra are nearly identical, confirming the absence of the linear peptide in the folding mixture (even a residual presence of the reduced peptide would have altered the isotopic pattern in the mass spectrum, as indicated in Supporting Information Figure S2b). Our work supports the use of high-resolution FT-MS as a diagnostic tool in assessing the quality of folded peptides having identical (or overlapping) HPLC retention times as the linear or partially reduced peptide.

To further evaluate the effect of the preformed diselenide cross-link on oxidative folding of GVIA, folding reactions were carried in the presence of a denaturing agent, 8 M urea. Figure 3b illustrates the steady-state accumulation of natively folded GVIA and Sec-GVIA analogues in the presence of 8 M urea. The amount of accumulation of natively folded peptides of GVIA and Sec-GVIA analogues is decreased, and the order of accumulation of the natively folded species for the Sec-GVIA analogue remained the same as observed during folding without denaturant. The decrease of yield of natively folded species for GVIA and Sec-GVIA analogues in 8 M urea could be ascribed in part to a loss of tertiary interactions under denaturing conditions. Interestingly, GVIA[C1U,C16U] and GVIA[C15U,C26U] have an additional HPLC peak with an oxidation state identical to that of the natively folded species (the observed masses were 3139.3 and 3139.5, respectively). Oxidative folding of the wild-type GVIA was devoid of predominant non-natively folded species in the presence of 8 M urea, as judged from the HPLC elution profile. These findings suggest that the diselenide cross-links may not only improve the yield of natively folded species but also affect the folding pathways. These data confirm the site-specific effects of the diselenide bridges on oxidative folding.

NMR-Based Disulfide Mapping. Disulfide mapping of Sec-GVIA analogues was carried out using the NMR-based method, recently described by Walewska et al. (*59*, *16*). The NMR-based mapping of disulfides, in the case of three-disulfide containing peptides, mainly relies upon observation of cross-disulfide

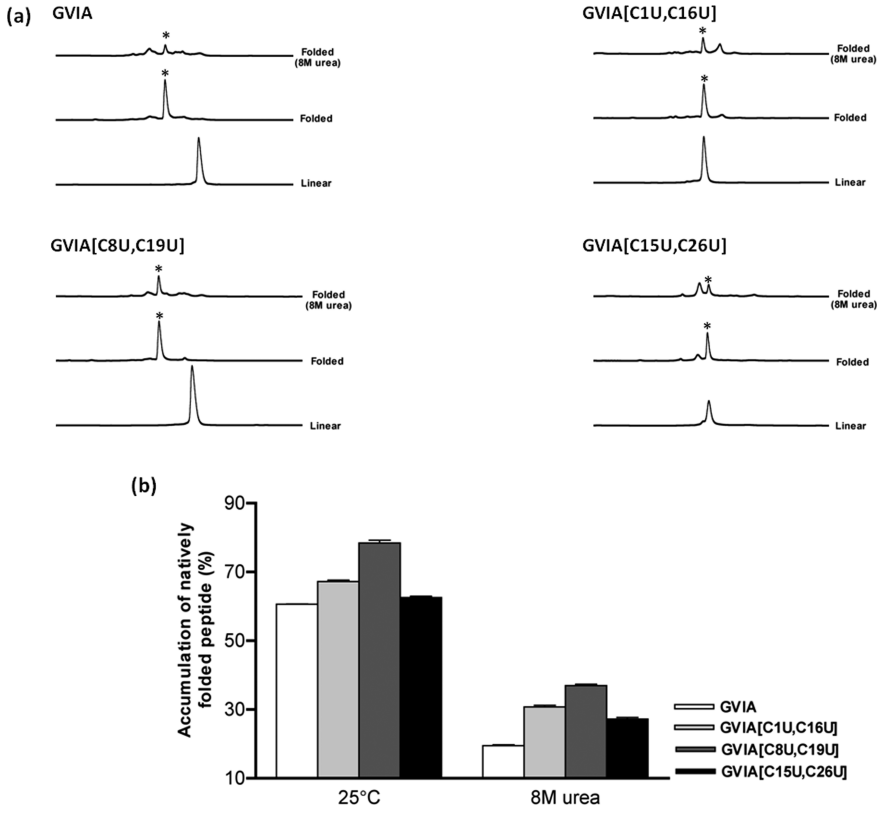

FIGURE 3: Synthesis and oxidative folding of GVIA and Sec-GVIA analogues. (a) RP-HPLC elution profiles of the linear/reduced species and the folding reactions carried out at room temperature and in the absence or presence of 8 M urea. Linear Sec-GVIA analogues contain a diselenide bridge, preformed during the processing of synthetic peptide. The folded peptide profile corresponds to the oxidative folding at steady state. The asterisk indicates the natively folded peptide. (b) Accumulation of natively folded peptide during oxidative folding at steady state, room temperature, and 8 M urea. Error bars represent the standard error of mean, derived from four independent experiments.

$H^{\alpha}/H^{\beta 1}/H^{\beta 2}$ NOESY cross-peaks across selectively labeled cysteines. The preformed diselenide bridge restricts the possible number of disulfide connectivites in three disulfide-containing peptides to three distinct possibilities.

To achieve the disulfide mapping for all three Sec-GVIA analogues, position-specific $^{15}N/^{13}C$-labeled cysteines were introduced during the chemical synthesis. GVIA[C1U,C16U] contained labeled cysteines at Cys8 and Cys19, GVIA[C8U,C19U] contained labeled cysteines at Cys15 and Cys26, and GVIA-[C15U,C26U] contains labeled cysteines at Cys1 and Cys16. Figure 4 shows heteronuclear NMR spectra of Sec-GVIA analogues. Two-dimensional [^{13}C,^{1}H] HSQC experiments were performed to identify labeled Cys residues, and the corresponding methine and methylene protons were assigned using the reported chemical shift values of GVIA. Two-dimensional ^{13}C-edited NOESY were recorded to identify cross-disulfide NOEs across interresidual $H^{\alpha}/H^{\beta 1}/H^{\beta 2}$ protons to confirm the disulfide bridge between labeled Cys residues. Two NOEs were observed across H^{β}/H^{β} protons of labeled cysteines in GVIA-[C1U,C16U], six NOEs across H^{β}/H^{β} protons of labeled cysteines in GVIA[C8U,C19U], and five NOEs across H^{α}/H^{β} and H^{α}/H^{α} protons of labeled cysteines in GVIA[C15U,C26U], confirming the presence of a disulfide bond between labeled cysteine residues in Sec-GVIA analogues. In the case of GVIA-[C15U,C26U], strong interresidue H^{α}/H^{β} and H^{α}/H^{α} NOEs are present while H^{β}/H^{β} NOEs are absent, perhaps due to the motional averaging about the disulfide (S−S) bond. The refined GVIA structure suggests that the disulfide Cys1-Cys16 exists in two different confirmations (*46*, *48*), indicating the motion about the disulfide bond and consequently affecting the orientation of methylene protons. Mass spectrometric data of folded Sec-GVIA analogues confirm the formation of the remaining disulfide bridge during oxidative folding. Thus, the disulfide connectivity in all tof he Sec-GVIA analogues, as revealed by the integrated approach, is between Cys1-Cys16, Cys8-Cys19, and Cys15-Cys26, which is identical to that of disulfide pairing in GVIA.

Peptide Mapping of Folding Intermediates. Disulfide mapping of the non-natively folded species of GVIA[C1U, C16U] and GVIA[C15U,C26U] was achieved using the proteolytic digestion strategy. The presence of four tryptic cleavage sites and three chymotryptic cleavage sites in GVIA allowed peptide mapping of the non-natively folded species. Figure 5a illustrates disulfide mapping of the non-natively folded GVIA[C1U,C16U] using trypsin. The tryptic digest of the non-natively folded GVIA[C1U,C16U] yielded closely migrating fragments with masses of 1269 and 1907 Da. These two masses could be ascribed to peptide fragments as rationalized in Figure 5a, confirming the disulfide connectivity in non-natively folded GVIA[C1U,C16U] as Cys8-Cys15 and Cys19-Cys26. Similarly, Figure 5b shows disulfide mapping of the non-natively folded GVIA[C15U, C26U] using chymotrypsin. The chymotryptic digest of non-natively folded GVIA[C15U,C26U] yielded fragments with masses of 1337 and 1821 Da. These two masses could be ascribed to peptide fragments as rationalized in Figure 5b, confirming the disulfide connectivity in non-natively folded GVIA[C15U,C26U] as Cys1-Cys8 and Cys16-Cys19. Noteworthy, the natively folded species are intact during enzymatic digestion due to their compact structure, further supporting the usefulness of NMR-based disulfide mapping.

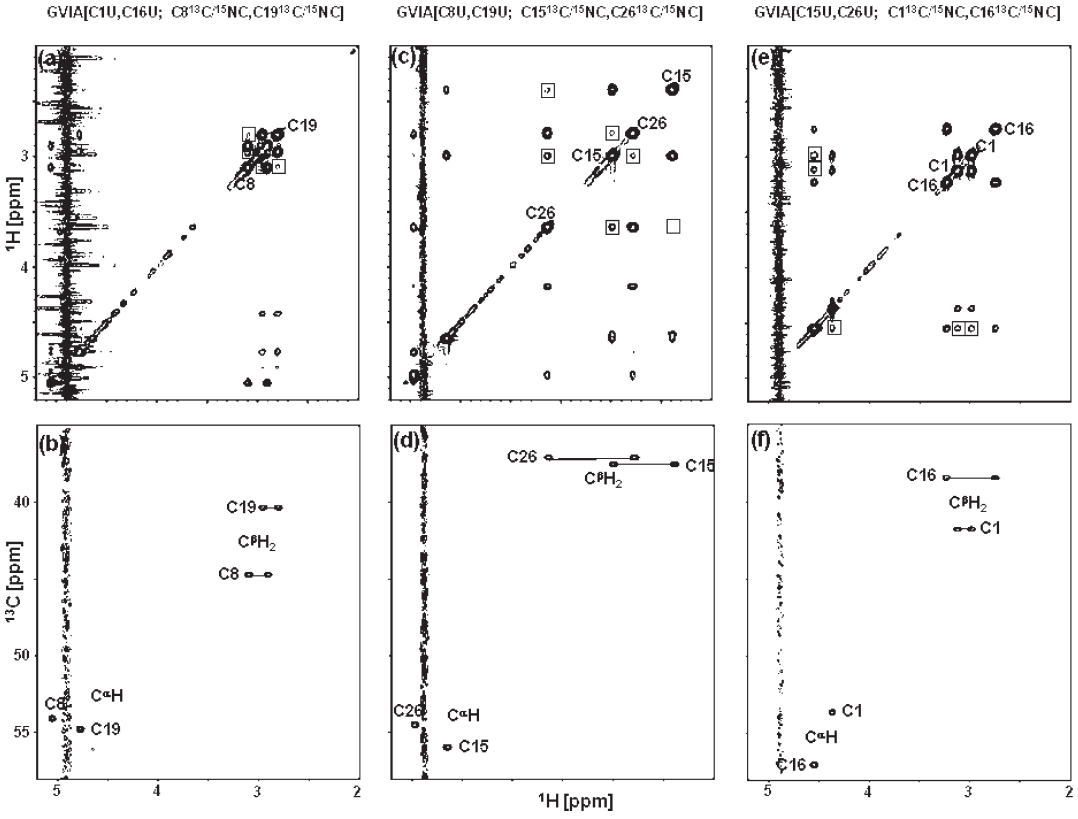

FIGURE 4: NMR-based disulfide mapping in Sec-GVIA analogues. Alignment of 2D F2-^{13}C-edited [^{1}H,^{1}H] NOESY (panels a, c, and e) with corresponding 2D [^{13}C,^{1}H] HSQC (panels b, d, and f) spectra of Sec-GVIA analogues: GVIA[C1U,C16U] (panels a and b), GVIA[C8U,C19U] (panels c and d), and GVIA[C15U,C26U] (panels e and f). Nondegenerate Cys C$^{\beta}$H$_2$ are connected with a line, and NOE cross-peaks confirming the disulfide bond between labeled cysteines are boxed. NOE between C1$^{\alpha}$H/C16$^{\alpha}$H in GVIA[C15U,C26U] is detected on the sharp C1$^{\alpha}$H signal only and not on the broader C16$^{\alpha}$H signal. The NOEs not labeled are assigned as intra-cysteine or from unassigned proximal protons, which pose no problems in disulfide mapping. All have been rationalized with the GVIA structure (*46*).

Folding Kinetics. The position-specific replacement of a disulfide bridge by the diselenide bridge imposes topological and conformational restrictions of the peptide chain in the reduced form that are present prior to the formation of the disulfide bridges. To better characterize the oxidative folding mechanism of the Sec-GVIA analogues, we studied folding kinetics and thermodynamics in the presence of the appropriate redox buffers. Figure 6a shows the RP-HPLC elution profile of the oxidative folding of GVIA and Sec-GVIA analogues quenched at appropriate time points. An accumulation of the native species was rapid for all three Sec-GVIA analogues compared to unsubstituted GVIA (Sec-GVIA analogues require formation of two disulfide bridges, whereas the wild-type GVIA requires the formation of three disulfide bonds). Figure 6b illustrates the kinetics of accumulation of native species in GVIA and Sec-GVIA analogues. Table 1 provides the rate constant for accumulation of natively folded GVIA and Sec-GVIA analogues during folding. Figure 6c highlights the importance of the diselenide cross-link on the folding kinetics of GVIA. During the early folding events of GVIA[C1U,C16U] and GVIA[C15U, C26U], the non-natively folded species is significantly accumulated, but the natively folded species predominates at the equilibrium (see Figure 6a and Figure S3, Supporting Information). Noteworthy, the non-natively folded species possess the smaller disulfide loops compared to the three distinct possible disulfide isomers of GVIA[C1U,C16U] and GVIA[C15U, C26U].

Table 2 summarizes the steady-state accumulation of the native and non-natively folded species under native and denaturing folding conditions. It is apparent from Table 2 that the accumulation of non-natively folded species decreases the overall yield of the natively folded peptides. The formation of smaller size disulfide loops favors the accumulation of non-natively folded species.

Figure 7 summarizes results derived from the oxidative folding of GVIA and Sec-GVIA analogues and also demonstrates the site-specific effect of the diselenide cross-link on oxidative folding of GVIA. Incorporation of site-specific selenocysteine residues has a significant impact on the oxidative folding mechanism of ω-conotoxin GVIA: the introduction of a diselenide bridge decreases the folding time required to produce the native-like species and improves folding yields, independent of the position of the diselenide bridge. However, in detail, the folding pathway for each Sec-GVIA analogue differs; the preformation of each diselenide specifically influences the orientation of the remaining thiol groups differentially.

Biological Activity. The NMR results demonstrate that the Sec-GVIA peptides fold properly, which predicts that each analogue should block N-type channels like GVIA. This was tested by applying each peptide at 1 μM to HEK293 cells transiently expressing N-type channels along with the ss_{2a} and $\alpha_2\delta$ subunits (*54*). Because of the slow blocking kinetics in the presence of millimolar divalent cations (*60*), we used an isochronic measurement to assess the block of N-current by each peptide (*61*). Figure 8 shows that a 16 min application of each Sec-GVIA peptide yielded almost complete block that was similar to GVIA. On average the percentage block was 98.5 $\pm$ 1.0 ($\pm$SD) for GVIA (n = 4), 98.7 $\pm$ 0.1 for GVIA[C1U,C16U]

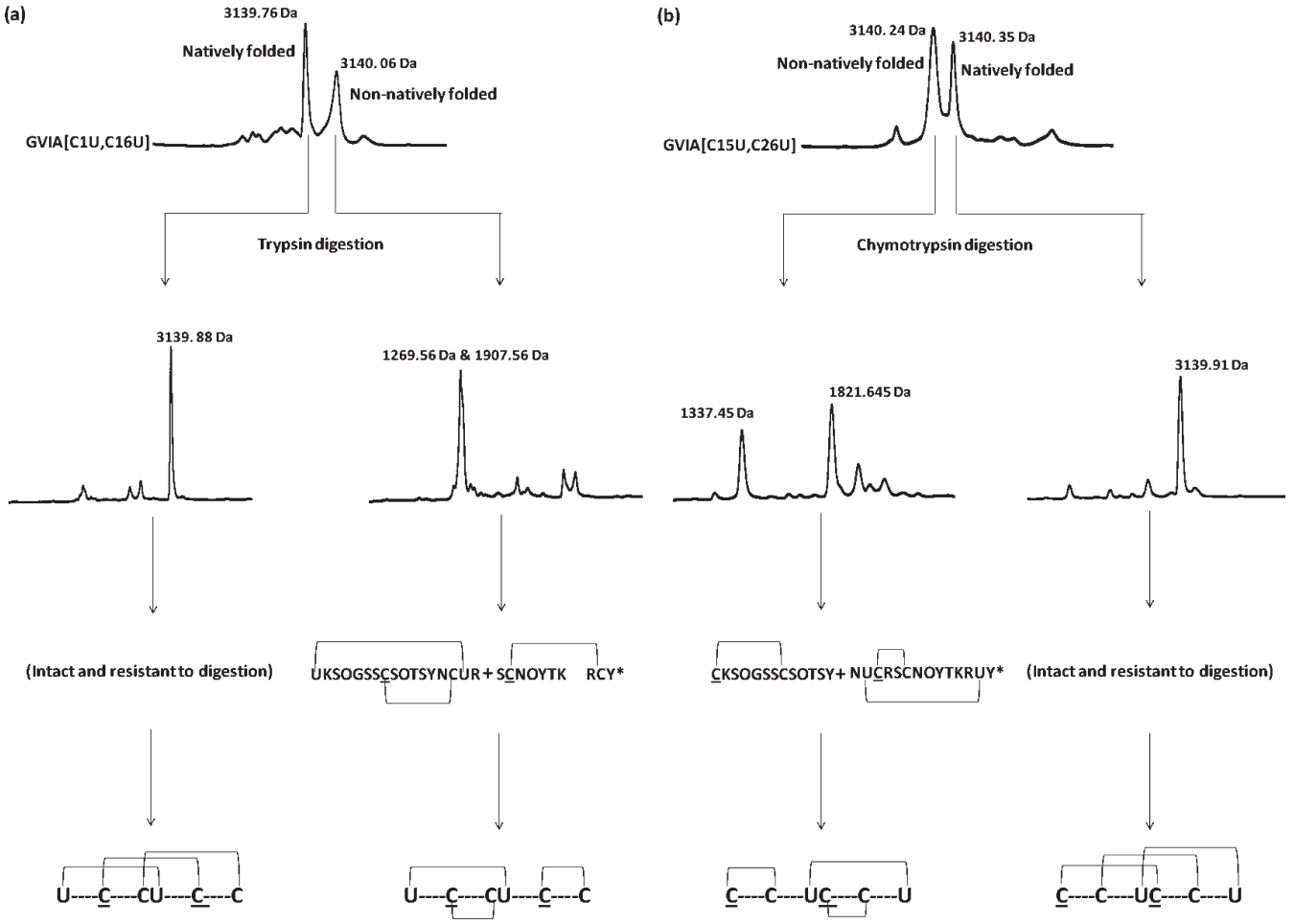

FIGURE 5: Disulfide mapping of non-natively folded peptides using proteolysis. (a) RP-HPLC elution profiles of folded GVIA[C1U,C16U] in the presence of 8 M urea and elution profile of the corresponding enzymatic digest using trypsin. (b) RP-HPLC elution profiles of folded GVIA[C15U,C26U] in the presence of 8 M urea and elution profile of the corresponding enzymatic digest using chymotrypsin. Disulfide topology in non-natively folded peptides was deduced using the observed mass of the enzymatic digest as rationalized in the figure, and observed mass in MALDI-MS was also indicated. (Note: C and * corresponds to labeled cysteine and C-terminal amidation, respectively. The diselenide bond exists prior to folding in linear Sec-GVIA analogues, and disulfide topology of natively folded peptide was derived using the integrated disulfide mapping approach as mentioned in Figure 4).

($n = 4$), 96.6 ± 1.7 for GVIA[C8U,C19U] ($n = 4$), and 96.5 ± 0.7 for GVIA[C15U,C26U] ($n = 5$). A small residual (unblocked) current was observed in each peptide after 16 min application (1 μM) and likely results from slow block in the presence of 5 mM Ba^{2+} used to record these currents (*60*, *61*). ANOVA analysis revealed no significant difference between the block induced by GVIA and GVIA[C1U,C16U] or GVIA[C8U,C19U], as well as among Sec-GVIA analogues. However, there was a difference between GVIA and GVIA[C15U,C26U] ($p < 0.05$). It is possible that GVIA[C15U,C26U] blocks slightly more slowly than GVIA, which would explain the significantly larger current at our 16 min time point. A more detailed evaluation of these peptides on voltage-dependent calcium currents is presently underway to address this and other issues. Together, our results demonstrate that all of the Sec-GVIA analogues are effective N-channel blockers.

Intracranial injection of the folded GVIA and Sec-GVIA analogues in mice elicited a shaking syndrome. Injected mice were persistently shaking their body a few minutes after injection. Prolongation of the persistent tremor is observed to be dose dependent, and at 1 nmol the behavior lasted for more than a day, with the mice being able to carry out normal functions although they were shaking. At higher concentrations, mice also exhibit a passive behavior with a backward leg extension. The similar behavioral phenotypes exhibited by GVIA and Sec-GVIA analogues upon intracranial injection in mice are consistent with the isomorphic replacement of cysteine by selenocysteine.

DISCUSSION

In this study, we assess the effects of substituting a diselenide for a native disulfide cross-link in the well-characterized inhibitory cystine knot peptide, ω-conotoxin GVIA. A diselenide was substituted for each of the three native disulfides, and the resulting selenocysteine-containing analogues were evaluated for whether the substitution affected either oxidative folding or/and function. The cross-linking pattern of each folded analogue of ω-conotoxin GVIA (containing a diselenide and two disulfides) was determined by NMR.

ω-Conotoxin GVIA is a well-characterized pore blocker of voltage-gated calcium channels with high affinity for the $Ca_V2.2$ subtype (*31*, *36*, *37*, *54*). Thus, one apparent advantage of using ω-GVIA as a model for testing the diselenide substitution was an easy and sensitive assessment of this approach on the bioactivity of the ICK-motif containing peptide. Electrophysiological experiments using HEK293 cells expressing the $Ca_V2.2$ channel demonstrated that all three Sec analogues of ω-conotoxin GVIA

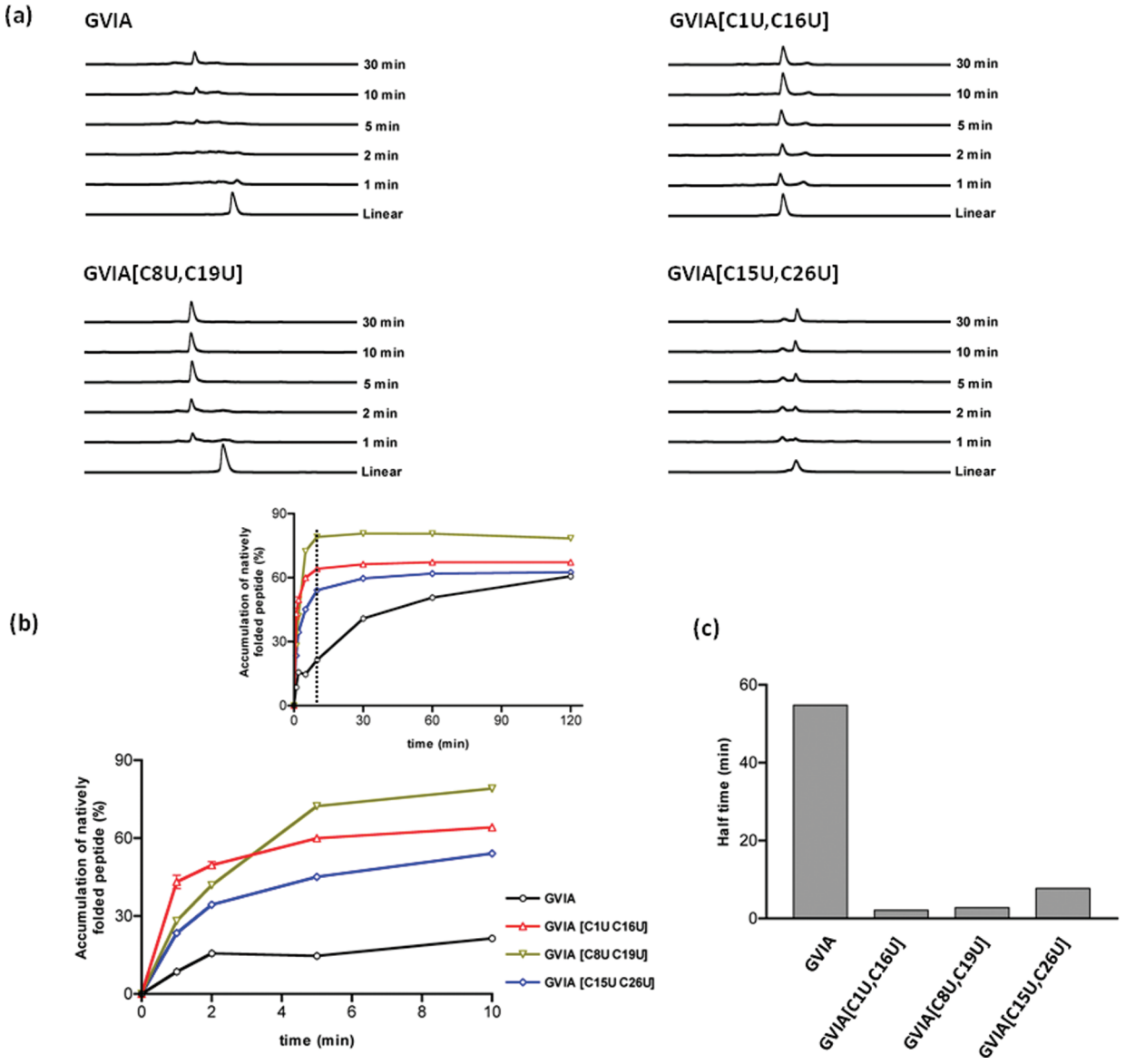

FIGURE 6: Folding kinetics of GVIA and Sec-GVIA analogues. (a) Reverse-phase C_{18} analytical HPLC elution profiles of the oxidative folding pathway. Reactions were quenched by acidification at regular intervals of time and analyzed using chromatography. The major peak in the profile indicates the natively folded peptide. (b) The accumulation of folded peptides was plotted against the regular intervals of time. Rate constants were obtained by fitting the experimental points to a single exponential fit. (c) Bar graph summarizing the time required to fold 50% of the natively folded species.

Table 1: Rate Constant (min^{-1}) of Oxidative Folding of Natively Folded Peptide in GVIA and Sec-GVIA at Different Experimental Conditions

peptide	25 °C	8 M urea
GVIA	0.049 ± 0.005	0.111 ± 0.009[a]
GVIA[C1U,C16U]	0.912 ± 0.061	0.747 ± 0.034
GVIA[C8U,C19U]	0.407 ± 0.011	0.202 ± 0.008
GVIA[C15U,C26U]	0.392 ± 0.026	0.227 ± 0.013

[a]Accumulation of natively folded GVIA was not observed during initial time points of oxidative folding in the presence of 8 M urea).

are fully functional compared to native ω-conotoxin GVIA. The *in vivo* functional activity of the Sec-GVIA analogues was not detectably different from ω-GVIA. Such benign effects of disulfide to diselenide were previously observed in other *Conus* peptides, namely, α- and μ-selenoconopeptides targeting nicotinic acetylcholine receptors and voltage-gated sodium channels, respectively (*15*, *16*). These examples add to a growing list of bioactive peptides containing diselenide bridges (*62*) and encourage further efforts to explore the selenopeptide strategy for discovery efforts and structure/function studies of disulfide-rich peptides (*63*).

Marked differences with respect to oxidative folding between Sec-GVIA analogues and ω-GVIA were observed. For all three Sec analogues, the kinetics of folding were significantly faster and the yields greater. The best yield was obtained when the second disulfide linkage (Cys8-Cys19) was replaced by a diselenide (an increase to 78%). The effects of diselenide bridges on folding kinetics were striking; it took significantly longer to fold ω-GVIA ($t_{1/2}$ > 50 min) than any of the Sec-GVIA analogues ($t_{1/2}$ < 10 min). Thus, substituting a diselenide for a native disulfide linkage in GVIA had no detectable effect on function but a marked acceleration in the kinetics of folding and an increase in yield of the properly folded analogue. Our proof-of-concept findings with Sec-GVIA are encouraging to apply the diselenide replacement to more difficult to chemically synthesize and oxidized ICK peptides, such as μO- or δ-conotoxins.

Table 2: Accumulation of Natively and Non-Natively Folded Sec-GVIA Analogues at Steady State under Different Folding Conditions[a]

Sec-GVIA analogues	disulfide isomers	fraction of natively and non-natively folded species		loop sizes of disulfides
		25 °C	8 M urea	
GVIA[C1U,C16U]	8−15, 19−26	14.5	34.3	6, 6
	8−19, 15−26	67.2	30.8	10, 10
GVIA[C8U,C19U]	**1−16, 15−26**	78.4	37.0	14, 10
GVIA[C15U,C26U]	1−8, 16−19	25.2	41.5	6, 2
	1−16, 8−19	62.5	27.4	14, 10

[a]Note: native-like disulfide connectivity is highlighted in bold font.

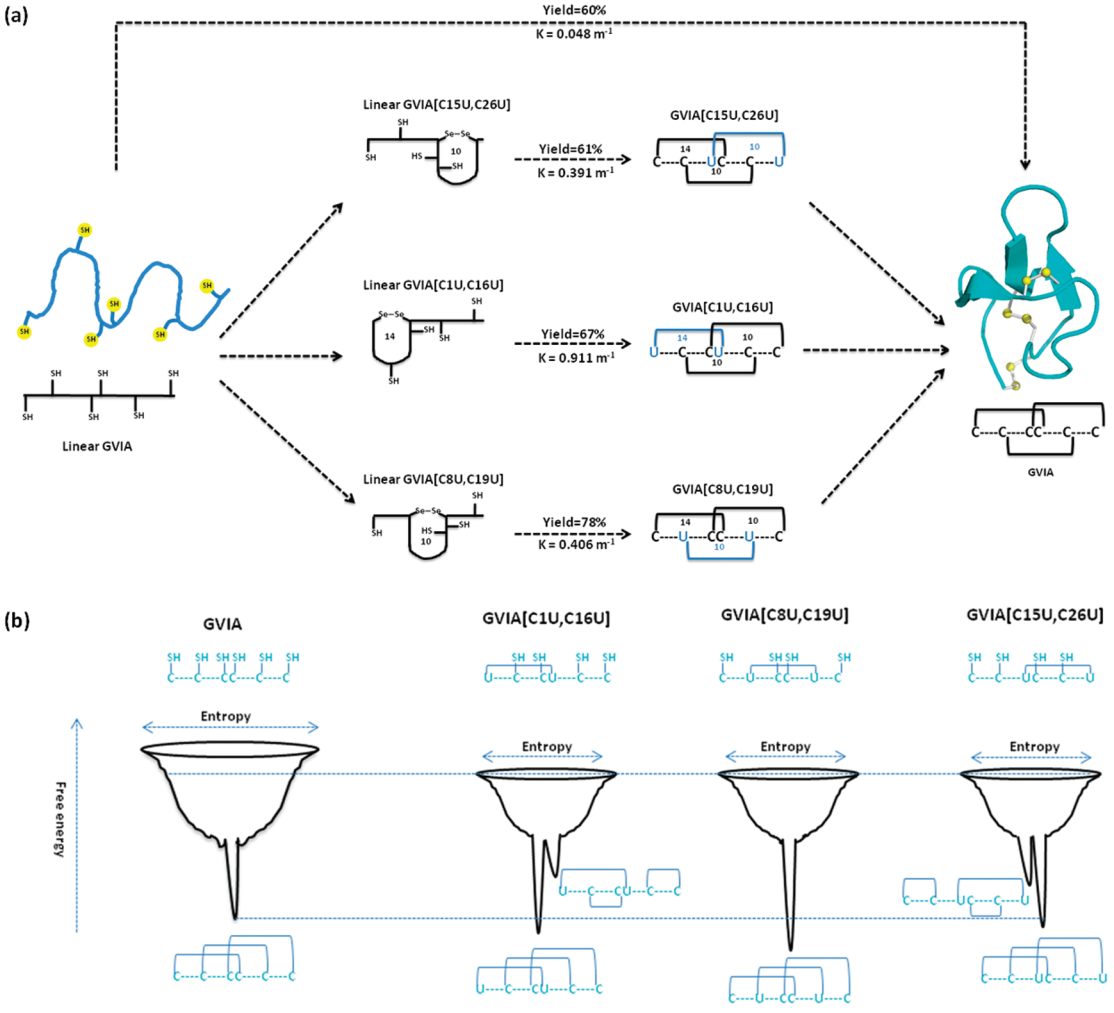

FIGURE 7: Schematic illustration of the oxidative folding of GVIA and Sec-GVIA analogues. (a) The topology of Sec-GVIA analogues is presented, and the number of residues involved in inter-cysteine or inter-selencysteine loops is also indicated. Folding yield and rates were derived from steady-state and folding kinetics experiments, respectively. (Note: rate constants for the natively folded peptides in Sec-GVIA analogues can be correlated with loop sizes of the corresponding disulfides formed during oxidative folding.) (b) Folding funnel representation of the site-specific effect of diselenide bridges on oxidative folding of GVIA. Disulfide connectivity of natively and non-natively folded Sec-GVIA analogues observed during the folding reactions is also emphasized.

Thermodynamic and kinetic studies on Sec-GVIA analogues emphasize the importance of loop sizes of disulfides/diselenides in increasing the yield and rate of accumulation of the natively folded peptides. The larger the size of a preformed diselenide loop, the faster the rate of accumulation of natively folded peptide. Effectiveness of improving the folding yield by site-specific incorporation of selenocysteine may depend on the formation of non-native disulfides, which also depends on the loop sizes of all the remaining possible disulfide connectivities (three distinct combinations exist for forming two disulfide bridges). The possibility of forming small disulfide loops in GVIA[C1U,C16U] and GVIA[C15U,C26U] resulted in the accumulation of non-natively folded peptides, decreasing the yield of forming the natively folded species. Comparable and larger size of non-native disulfide loops in GVIA[C8U,C19U] may have precluded the accumulation of the non-natively folded species, thus increasing the overall folding yield. These findings suggest how to design analogues of cysteine-rich peptides with site-specific incorporation of selenocysteine to rationally engineer the oxidative folding pathways. More studies are clearly needed

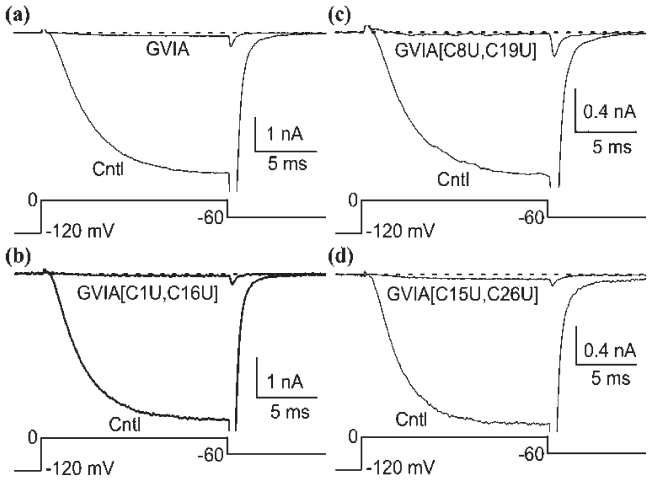

FIGURE 8: The blocking effect of GVIA and Sec-GVIA analogues on the N-type calcium channel. N-type currents were recorded before (control, Cntl) and after 16 min application of 1 μM peptide analogues (as indicated). Voltage protocol is shown at the bottom of each panel. The tail currents on the control records were clipped to highlight the block of step current.

to generalize these findings to other than the ICK disulfide scaffolds.

Our results also support broader use of selectively labeled $^{13}C/^{15}N$ cysteine residues for disulfide mapping by means of NMR. In general, the following rules may assist preferential incorporation of labeled cysteine in disulfide-rich peptides and subsequent efficient disulfide mapping. (1) Cysteines with well-dispersed H^{β} chemical shifts should be first selected for labeling as they potentially can provide the largest number of cross-disulfide NOEs. (2) In the case of degenerate H^{β} chemical shifts, intraresidue degenerate H^{β}s should be preferred over inter-residue degenerate H^{β}s for labeling. High-resolution NMR spectroscopy together with careful selection for incorporation of $^{13}C/^{15}N$-labeled cysteine residues in disulfide-rich peptides should assist rapid disulfide mapping. Recently, ^{77}Se NMR was used to determine a diselenide connectivity in a selenopeptide analogue of spider toxin κ-ACTX-Hv1c (*64*), further confirming that NMR-based methods may offer an attractive alternative to a traditional mapping of disulfide bridges by partial reduction, followed by a proteolytic or chemical fragmentation and mass spectrometry analysis.

The results demonstrate that diselenide substitution for a native disulfide bond may be a feasible strategy for producing ICK peptide analogues that retain the biological activity of the native peptide but have improved folding kinetics and yields. The improved folding kinetics could be particularly beneficial in those cases where ICK peptides fold very inefficiently and tend to aggregate during the folding reaction. These are all candidates for using the diselenide strategy. We are presently determining whether a dramatic improvement in yield can be attained in these cases. The ICK peptides comprise a structurally and functionally diverse group of bioactive peptides, including neurotoxins, protease inhibitors, antiviral cyclotides, and antimicrobial peptides. Research on ICK peptides involves drug discovery and preclinical/clinical development, validating this group of peptides as a rich source of new, potential first-in-class, biotherapeutics. Our work encourages using the integrated oxidative folding approach to study structure and function of the ICK peptides.

ACKNOWLEDGMENT

We thank Drs. Robert Schackmann and Scott Endicott from the DNA/Peptide Synthesis Core Facility at the University of Utah for the synthesis of peptides. The Pennsylvania Department of Health specifically disclaims responsibility for analyses, interpretations, and conclusions presented here. K.H.G. acknowledges the help of Dr. Chad C. Nelson and Dr. Krishna Parsawar of the Mass Spectrometry and Proteomic Core Facility at the University of Utah for generating theoretical mass spectra. We thank Prof. Ray Norton for critical reading of the manuscript. Conflict of Interest disclosure: B.M.O. is a cofounder of Cognetix, Inc.; G.B. is a cofounder of NeuroAdjuvants, Inc.

SUPPORTING INFORMATION AVAILABLE

One table (summary of KNOTTIN database analysis for three disulfide-containing ICK peptides) and three supplemental figures (Figure S1, HPLC and mass spectrometry analysis of the linear form of GVIA[C8U,C19U]; Figure S2, high-resolution mass spectrometry analysis of the folded species of GIVA-[C1U,C16U]; and Figure S3, folding kinetics of GVIA and Sec-GVIA analogues in the presence of 8 M urea). This material is available free of charge via the Internet at http://pubs.acs.org.

REFERENCES

1. Gray, W. R., Olivera, B. M., and Cruz, L. J. (1988) Peptide toxins from venomous *Conus* snails. *Annu. Rev. Biochem. 57*, 665–700.
2. Lehrer, R. I., Lichtenstein, A. K., and Ganz, T. (1993) Defensins: antimicrobial and cytotoxic peptides of mammalian cells. *Annu. Rev. Immunol. 11*, 105–128.
3. Ryan, C. A. (2006) Hand Book of Biologically Active Peptides, Academic Press, Elsiever, San Diego, CA.
4. Mouhat, S., Jouirou, B., Mosbah, A., De Waard, M., and Sabatier, J. M. (2004) Diversity of folds in animal toxins acting on ion channels. *Biochem. J. 378*, 717–726.
5. Olivera, B. M., Rivier, J., Clark, C., Ramilo, C. A., Corpuz, G. P., Abogadie, F. C., Mena, E. E., Woodward, S. R., Hillyard, D. R., and Cruz, L. J. (1990) Diversity of *Conus* neuropeptides. *Science 249*, 257–263.
6. Olivera, B. M. (1997) E. E. Just Lecture, 1996. *Conus* venom peptides, receptor and ion channel targets, and drug design: 50 million years of neuropharmacology. *Mol. Biol. Cell 8*, 2101–2109.
7. Molinski, T. F., Dalisay, D. S., Lievens, S. L., and Saludes, J. P. (2009) Drug development from marine natural products. *Nat. Rev. Drug Discov. 8*, 69–85.
8. Bulaj, G., and Walewska, A. (2009) Oxidative folding of single-stranded, disulfide-rich peptides, in Oxidative folding of peptides and proteins (Buchner, J., and Moroder, L., Eds.) pp 274−296, The Royal Society of Chemistry, Cambridge, U.K.
9. Arolas, J. L., Aviles, F. X., Chang, J. Y., and Ventura, S. (2006) Folding of small disulfide-rich proteins: clarifying the puzzle. *Trends Biochem. Sci. 31*, 292–301.
10. Bulaj, G., and Olivera, B. M. (2008) Folding of conotoxins: formation of the native disulfide bridges during chemical synthesis and biosynthesis of *Conus* peptides. *Antioxid. Redox Signaling 10*, 141–155.
11. DeLa Cruz, R., Whitby, F. G., Buczek, O., and Bulaj, G. (2003) Detergent-assisted oxidative folding of δ-conotoxins. *J. Pept. Res. 61*, 202–212.
12. Fiori, S., Pegoraro, S., Rudolph-Böhner, S., Cramer, J., and Moroder, L. (2000) Synthesis and conformational analysis of apamin analogues with natural and non-natural cystine/selenocystine connectivities. *Biopolymers 53*, 550–564.
13. Pegoraro, S., Fiori, S., Cramer, J., Rudolph-Böhner, S., and Moroder, L. (1999) The disulfide-coupled folding pathway of apamin as derived from diselenide-quenched analogs and intermediates. *Protein Sci. 8*, 1605–1613.
14. Pegoraro, S., Fiori, S., Rudolph-Böhner, S., Watanabe, T. X., and Moroder, L. (1998) Isomorphous replacement of cystine with selenocystine in endothelin: oxidative refolding, biological and conformational properties of [Sec3,Sec11,Nle7]-endothelin-1. *J. Mol. Biol. 284*, 779–792.

15. Armishaw, C. J., Daly, N. L., Nevin, S. T., Adams, D. J., Craik, D. J., and Alewood, P. F. (2006) α-Selenoconotoxins, a new class of potent alpha7 neuronal nicotinic receptor antagonists. *J. Biol. Chem. 281*, 14136–14143.
16. Walewska, A., Zhang, M. M., Skalicky, J. J., Yoshikami, D., Olivera, B. M., and Bulaj, G. (2009) Integrated oxidative folding of cysteine/selenocysteine containing peptides: improving chemical synthesis of conotoxins. *Angew. Chem., Int. Ed. Engl. 48*, 2221–2224.
17. Rees, D. C., and Lipscomb, W. N. (1982) Refined crystal structure of the potato inhibitor complex of carboxypeptidase A at 2.5 Å resolution. *J. Mol. Biol. 160*, 475–498.
18. Pallaghy, P. K., Nielsen, K. J., Craik, D. J., and Norton, R. S. (1994) A common structural motif incorporating a cystine knot and a triple-stranded beta-sheet in toxic and inhibitory polypeptides. *Protein Sci. 3*, 1833–1839.
19. Gelly, J. C., Gracy, J., Kaas, Q., Le-Nguyen, D., Heitz, A., and Chiche, L. (2004) The KNOTTIN website and database: a new information system dedicated to the knottin scaffold. *Nucleic Acids Res. 32*, 156–159.
20. Gracy, J., Le-Nguyen, D., Gelly, J. C., Kaas, Q., Heitz, A., and Chiche, L. (2008) KNOTTIN: the knottin or inhibitor cystine knot scaffold in 2007. *Nucleic Acids Res. 36*, 314–319.
21. Norton, R. S., and Pallaghy, P. K. (1998) The cystine knot structure of ion channel toxins and related polypeptides. *Toxicon 36*, 1573–1583.
22. Terlau, H., and Olivera, B. M. (2004) *Conus* venoms: a rich source of novel ion channel-targeted peptides. *Physiol. Rev. 84*, 41–68.
23. Olivera, B. M., Walker, C., Cartier, G. E., Hooper, D., Santos, A. D., Schoenfeld, R., Shetty, R., Watkins, M., Bandyopadhyay, P., and Hillyard, D. R. (1999) Speciation of cone snails and interspecific hyperdivergence of their venom peptides. Potential evolutionary significance of introns. *Ann. N.Y. Acad. Sci. 870*, 223–237.
24. Duda, T. F., Jr., and Palumbi, S. R. (1999) Molecular genetics of ecological diversification: duplication and rapid evolution of toxin genes of the venomous gastropod *Conus*. *Proc. Natl. Acad. Sci. U.S.A. 96*, 6820–6823.
25. Olivera, B. M., McIntosh, J. M., Cruz, L. J., Luque, F. A., and Gray, W. R. (1984) Purification and sequence of a presynaptic peptide toxin from *Conus geographus* venom. *Biochemistry 23*, 5087–5090.
26. Shon, K. J., Stocker, M., Terlau, H., Stühmer, W., Jacobsen, R., Walker, C., Grilley, M., Watkins, M., Hillyard, D. R., Gray, W. R., and Olivera, B. M. (1998) κ-Conotoxin PVIIA is a peptide inhibiting the shaker K^+ channel. *J. Biol. Chem. 273*, 33–38.
27. Shon, K. J., Hasson, A., Spira, M. E., Cruz, L. J., Gray, W. R., and Olivera, B. M. (1994) δ-Conotoxin GmVIA, a novel peptide from the venom of *Conus gloriamaris*. *Biochemistry 33*, 11420–11425.
28. McIntosh, J. M., Hasson, A., Spira, M. E., Gray, W. R., Li, W., Marsh, M., Hillyard, D. R., and Olivera, B. M. (1995) A new family of conotoxins that blocks voltage-gated sodium channels. *J. Biol. Chem. 270*, 16796–16802.
29. Fainzilber, M., van der Schors, R., Lodder, J. C., Li, K. W., Geraerts, W. P., and Kits, K. S. (1995) New sodium channel-blocking conotoxins also affect calcium currents in *Lymnaea* neurons. *Biochemistry 34*, 5364–5371.
30. Olivera, B. M., Gray, W. R., Zeikus, R., McIntosh, J. M., Varga, J., Rivier, J., de Santos, V., and Cruz, L. J. (1985) Peptide neurotoxins from fish-hunting cone snails. *Science 230*, 1338–1343.
31. Olivera, B. M., Miljanich, G. P., Ramachandran, J., and Adams, M. E. (1994) Calcium channel diversity and neurotransmitter release: the ω-conotoxins and ω-agatoxins. *Annu. Rev. Biochem. 63*, 823–867.
32. Olivera, B. M. (2000) ω-Conotoxin MVIIA: from marine snail venom to analgesic drug, in Drugs from the sea (Fusetani, N., Ed.) Karger, Basel.
33. Miljanich, G. P. (2004) Ziconotide: neuronal calcium channel blocker for treating severe chronic pain. *Curr. Med. Chem. 11*, 3029–3040.
34. Cruz, L. J., and Olivera, B. M. (1986) Calcium channel antagonists. ω-Conotoxin defines a new high affinity site. *J. Biol. Chem. 261*, 6230–6233.
35. McCleskey, E. W., Fox, A. P., Feldman, D. H., Cruz, L. J., Olivera, B. M., Tsien, R. W., and Yoshikami, D. (1987) ω-Conotoxin: direct and persistent blockade of specific types of calcium channels in neurons but not muscle. *Proc. Natl. Acad. Sci. U.S.A. 84*, 4327–4331.
36. Reynolds, I. J., Wagner, J. A., Snyder, S. H., Thayer, S. A., Olivera, B. M., and Miller, R. J. (1986) Brain voltage-sensitive calcium channel subtypes differentiated by ω-conotoxin fraction GVIA. *Proc. Natl. Acad. Sci. U.S.A. 83*, 8804–8807.
37. Hillyard, D. R., Monje, V. D., Mintz, I. M., Bean, B. P., Nadasdi, L., Ramachandran, J., Miljanich, G., Azimi-Zoonooz, A., McIntosh, J. M., Cruz, L. J., and Olivera, B. M. (1992) A new Conus peptide ligand for mammalian presynaptic Ca^{2+} channels. *Neuron 9*, 69–77.
38. Adams, M. E., and Olivera, B. M. (1994) Neurotoxins: overview of an emerging research technology. *Trends Neurosci. 17*, 151–155.
39. Horne, A. L., and Kemp, J. A. (1991) The effect of omega-conotoxin GVIA on synaptic transmission within the nucleus accumbens and hippocampus of the rat in vitro. *Br. J. Pharmacol. 103*, 1733–1739.
40. Takahashi, T., and Momiyama, A. (1993) Different types of calcium channels mediate central synaptic transmission. *Nature 366*, 156–158.
41. Price-Carter, M., Gray, W. R., and Goldenberg, D. P. (1996) Folding of ω-conotoxins. 1. Efficient disulfide-coupled folding of mature sequences in vitro. *Biochemistry 35*, 15537–15546.
42. Price-Carter, M., Gray, W. R., and Goldenberg, D. P. (1996) Folding of ω-conotoxins. 2. Influence of precursor sequences and protein disulfide isomerase. *Biochemistry 35*, 15547–15557.
43. Price-Carter, M., Hull, M. S., and Goldenberg, D. P. (1998) Roles of individual disulfide bonds in the stability and folding of an ω-conotoxin. *Biochemistry 37*, 9851–9861.
44. Price-Carter, M., Bulaj, G., and Goldenberg, D. P. (2002) Initial disulfide formation steps in the folding of an ω-conotoxin. *Biochemistry 41*, 3507–3519.
45. Davis, J. H., Bradley, E. K., Miljanich, G. P., Nadasdi, L., Ramachandran, J., and Basus, V. J. (1993) Solution structure of ω-conotoxin GVIA using 2-D NMR spectroscopy and relaxation matrix analysis. *Biochemistry 32*, 7396–7405.
46. Skalicky, J. J., Metzler, W. J., Ciesla, D. J., Galdes, A., and Pardi, A. (1993) Solution structure of the calcium channel antagonist ω-conotoxin GVIA. *Protein Sci. 2*, 1591–1603.
47. Pallaghy, P. K., Duggan, B. M., Pennington, M. W., and Norton, R. S. (1993) Three-dimensional structure in solution of the calcium channel blocker ω-conotoxin. *J. Mol. Biol. 234*, 405–420.
48. Pallaghy, P. K., and Norton, R. S. (1999) Refined solution structure of ω-conotoxin GVIA: implications for calcium channel binding. *J. Pept. Res. 53*, 343–351.
49. Yoshikami, D., Bagabaldo, Z., and Olivera, B. M. (1989) The inhibitory effects of ω-conotoxins on Ca channels and synapses. *Ann. N.Y. Acad. Sci. 560*, 230–248.
50. Lampe, R. A., Lo, M. M., Keith, R. A., Horn, M. B., McLane, M. W., Herman, J. L., and Spreen, R. C. (1993) Effects of site-specific acetylation on ω-conotoxin GVIA binding and function. *Biochemistry 32*, 3255–3260.
51. Sato, K., Park, N. G., Kohno, T., Maeda, T., Kim, J. I., Kato, R., and Takahashi, M. (1993) Role of basic residues for the binding of ω-conotoxin GVIA to N-type calcium channels. *Biochem. Biophys. Res. Commun. 194*, 1292–1296.
52. Lew, M. J., Flinn, J. P., Pallaghy, P. K., Murphy, R., Whorlow, S. L., Wright, C. E., Norton, R. S., and Angus, J. A. (1997) Structure-function relationships of ω-conotoxin GVIA. Synthesis, structure, calcium channel binding, and functional assay of alanine-substituted analogues. *J. Biol. Chem. 272*, 12014–12023.
53. Flinn, J. P., Pallaghy, P. K., Lew, M. J., Murphy, R., Angus, J. A., and Norton, R. S. (1999) Roles of key functional groups in ω-conotoxin GVIA synthesis, structure and functional assay of selected peptide analogues. *Eur. J. Biochem. 262*, 447–455.
54. Yarotskyy, V., and Elmslie, K. S. (2009) {omega}-conotoxin GVIA alters gating charge movement of N-type (CaV2.2) calcium channels. *J. Neurophysiol. 101*, 332–340.
55. Yarotskyy, V., and Elmslie, K. S. (2007) Roscovitine, a cyclin-dependent kinase inhibitor, affects several gating mechanisms to inhibit cardiac L-type (Ca(V)1.2) calcium channels. *Br. J. Pharmacol. 152*, 386–395.
56. Harris, K. M., Flemer, S., Jr., and Hondal, R. J. (2007) Studies on deprotection of cysteine and selenocysteine side-chain protecting groups. *J. Pept. Sci. 13*, 81–93.
57. Hondal, R. J. (2009) Using chemical approaches to study selenoproteins-focus on thioredoxin reductases. *Biochim. Biophys. Acta 1790*, 1501–1512.
58. Besse, D., Siedler, F., Diercks, T., Kessler, H., and Morder, L. (1997) The redox potential of selenocysteine in unconstrained cyclic peptides. *Angew. Chem., Int. Ed. Engl. 36*, 883–885.
59. Walewska, A., Skalicky, J. J., Davis, D. R., Zhang, M. M., Lopez-Vera, E., Watkins, M., Han, T. S., Yoshikami, D., Olivera, B. M., and Bulaj, G. (2008) NMR-based mapping of disulfide bridges in cysteine-rich peptides: application to the m-conotoxin SxIIIA. *J. Am. Chem. Soc. 130*, 14280–14286.
60. Liang, H., and Elmslie, K. S. (2002) Rapid and reversible block of N-type calcium channels (CaV 2.2) by ω-conotoxin GVIA in the absence of divalent cations. *J. Neurosci. 22*, 8884–8890.
61. Boland, L. M., Morrill, J. A., and Bean, B. P. (1994) ω-Conotoxin block of N-type calcium channels in frog and rat sympathetic neurons. *J. Neurosci. 14*, 5011–5027.

62. Moroder, L. (2005) Isosteric replacement of sulfur with other chalcogens in peptides and proteins. *J. Pept. Sci. 11*, 187–214.
63. Muttenthaler, M., and Alewood, P. F. (2008) Selenopeptide chemistry. *J. Pept. Sci. 14*, 1223–1239.
64. Mobli, M, de Araújo, A. D., Lambert, L. K., Pierens, G. K., Windley, M. J., Nicholson, G. M., Alewood, P. F., and King, G. F. (2009) Direct visualization of disulfide bonds through diselenide proxies using ^{77}Se NMR spectroscopy. *Angew. Chem., Int. Ed. Engl. 48*, 9312–9314.